
SSM Meets Video Diffusion Models: Efficient Video Generation with Structured State Spaces

Yuta Oshima¹ Shohei Taniguchi¹ Masahiro Suzuki¹ Yutaka Matsuo¹

Abstract

Given the remarkable achievements in image generation through diffusion models, the research community has shown increasing interest in extending these models to video generation. Recent diffusion models for video generation have predominantly utilized attention layers to extract temporal features. However, attention layers are limited by their memory consumption, which increases quadratically with the length of the sequence. This limitation presents significant challenges when attempting to generate longer video sequences using diffusion models. To overcome this challenge, we propose leveraging state-space models (SSMs). SSMs have recently gained attention as viable alternatives due to their linear memory consumption relative to sequence length. In the experiments, we first evaluate our SSM-based model with UCF101, a standard benchmark of video generation. In addition, to investigate the potential of SSMs for longer video generation, we perform an experiment using the MineRL Navigate dataset, varying the number of frames to 64, 200, and 400. In these settings, our SSM-based model can considerably save memory consumption for longer sequences, while maintaining competitive FVD scores to the attention-based models. Our codes are available at <https://github.com/shim0114/SSM-Meets-Video-Diffusion-Models>.

1. Introduction

Expanding upon the early strides made in deep generative models, substantial research endeavors have been dedicated to the realm of video generation. Initial investigations within this domain primarily centered around frameworks includ-

ing variational autoencoders (VAE) (Kingma & Welling, 2013; Kim et al., 2019; Saxena et al., 2021; Yan et al., 2021) and generative adversarial networks (GAN) (Goodfellow et al., 2014; Vondrick et al., 2016; Tulyakov et al., 2018; Ge et al., 2022). These foundational studies laid the groundwork for subsequent advancements in this field.

Research on video generation using diffusion models (Sohl-Dickstein et al., 2015; Nichol & Dhariwal, 2021; Ho et al., 2020) is cutting-edge in the field of deep generative models. The success of image generation using diffusion models, notably Denoising Diffusion Probabilistic Models (DDPMs) (Ho et al., 2020), has sparked a surge in research on applying diffusion models to video generation. This trend has been exemplified by the emergence of video diffusion models (VDMs) (Ho et al., 2022b). By harnessing the substantial representational capacity inherent in diffusion models, their application to video generation has showcased impressive performance in modeling the dynamic and intricate nature of video content (Ho et al., 2022b; Singer et al., 2022; Ho et al., 2022a)

However, research on diffusion-model-based video generation faces significant challenges in terms of computational complexity with respect to temporal sequence length. In diffusion models for video generation, attention mechanisms (Vaswani et al., 2017) are employed to capture temporal relationships (Ho et al., 2022b; Singer et al., 2022; Ho et al., 2022a; Zhou et al., 2022; Blattmann et al., 2023). Unlike recurrent models, such as LSTM layers (Chung et al., 2014; Hochreiter & Schmidhuber, 1997), attention layers allow for parallel computations, making this method widely used. In early studies on diffusion models for video generation, such as VDMs, to capture temporal relationships across video frames, temporal attention layers were added subsequent to spatial attention layers within the architecture of diffusion models for image generation, as described in Figure 1 (a). However, the memory demands of attention layers, which scale with the square of the sequence length, present substantial challenges for extending these models to handle longer sequences. Although there have been many attempts to improve the memory efficiency of attention mechanisms (Shen et al., 2018; Kitaev et al., 2020; Wang et al., 2020), these methods tend to exhibit performance deteriora-

¹The University of Tokyo, 7-3-1, Hongo, Bunkyo-ku, Tokyo, Japan. Correspondence to: Yuta Oshima <yuta.oshima@weblab.t.u-tokyo.ac.jp>.

Preliminary work. Under review by the International Conference on Machine Learning (ICML). Do not distribute.

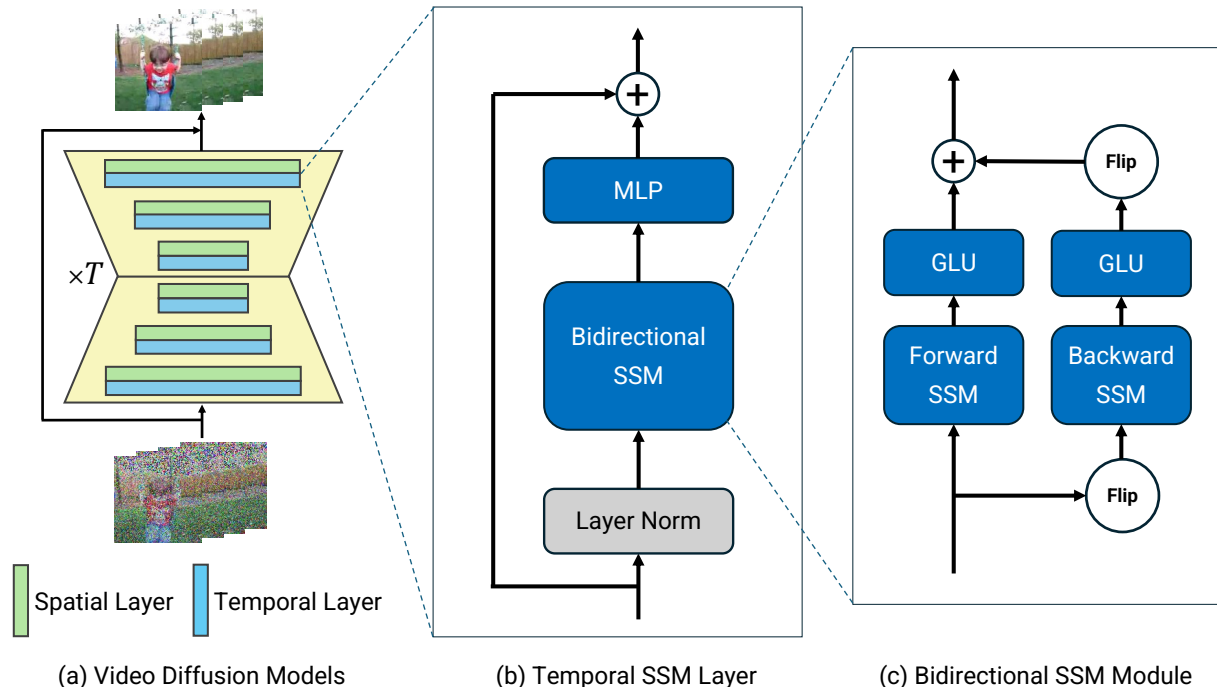


Figure 1. (a) U-Net based video diffusion models consist of spatial layers and temporal layers. (b) In our temporal SSM layer, we replace an attention module with a bidirectional SSM module + a dual-layer MLP in a traditional temporal layer in VDMs. (c) Details of a bidirectional SSM in our temporal SSM layer. Following common practices, GLU is used to intermix information across different dimensions of outputs from SSM. Element-wise summation is utilized to aggregate features from bidirectional SSMs.

tion compared to traditional attention mechanisms.

Recently, state-space models (SSMs) (Gu et al., 2020; 2021; 2022; Smith et al., 2023; Gu & Dao, 2023) have been identified as promising alternatives to attention mechanisms. A pioneering work by Gu et al. (2021) has enabled SSMs to capture long-term dependencies of sequential data, and their model, named the structured state space sequence model (S4), demonstrates superior performance in various benchmarks of sequence modeling. In contrast to attention mechanisms, SSMs can handle sequential data with linear complexities, so they are expected to overcome the fundamental limitation of attention-based models in many sequence modeling tasks.

Although subsequent studies have also shown that SSMs are effective across various domains (see 4.2), in the field of video generation, the application of SSMs has not been explored. This is because a methodology to effectively incorporate SSMs into video generation models, such as VDMs, has not been established. In fact, we have empirically observed that a naive approach that directly replace temporal attention layers of VDMs with SSMs works much worse than the original attention-based VDMs. To bridge this gap, in this paper, we investigate an effective approach to incorporate SSMs with video diffusion models. Our pro-

posed model is summarized in Figure 1. A key insight of our investigation is that using bidirectional SSMs is essential to achieve good performance for SSM-based VDMs. In addition, to capture complex nonlinear dynamics of video sequences, adding a multi-layer perceptron (MLP) after the bidirectional SSM is also very effective to improve the generative performance.

In the experiments, we demonstrate that by substituting temporal attention in video diffusion models with our temporal SSM layers, it is feasible to show competitive or even better generative performance in benchmarks of video generation, e.g., UCF101 (Soomro et al., 2012), in terms of the Fréchet Video Distance (FVD) (Unterthiner et al., 2018). Moreover, we additionally observe that our SSM-based model can be successfully trained with 400-frame videos of Min-eRL Navigate (Guss et al., 2019; Saxena et al., 2021) with eight A100 GPUs, while attention-based VDM cannot due to huge memory consumption. We also uncover critical factors that contribute to generative qualities when utilizing SSMs for video diffusion models in ablation study.

2. Background

In this section, we provide an overview of our initial understanding of diffusion models for video generation. Diffusion models were initially introduced by [Sohl-Dickstein et al. \(2015\)](#), and [Ho et al. \(2020\)](#) further advanced the field with the introduction of denoising diffusion probabilistic models (DDPMs). DDPMs introduced a practical training algorithm, particularly well-suited for image generation. Recent advancements in diffusion models for video generation involve the extension of the DDPM architecture to accommodate video data.

2.1. Denoising Diffusion Probabilistic Models (DDPMs)

In diffusion models, the forward process involves progressively diminishing the original data signal, \mathbf{x}_0 , by gradually introducing Gaussian noise as the diffusion time, t , advances. This sequence of transformations leads \mathbf{x}_0 to converge to pure Gaussian noise, represented as $\mathbf{x}_T \sim \mathcal{N}(\mathbf{x}_T; \mathbf{0}, \mathbf{I})$, at time T . In our study, t is treated as a discrete integer within the range $[0, T]$, although some studies have considered t as a continuous variable ([Song et al., 2021](#); [Kingma et al., 2021](#)). The forward process is governed by the following following Markov process:

$$q(\mathbf{x}_{1:T}|\mathbf{x}_0) = \prod_{t=1}^T q(\mathbf{x}_t|\mathbf{x}_{t-1}), \quad (1)$$

$$q(\mathbf{x}_t|\mathbf{x}_{t-1}) = \mathcal{N}(\mathbf{x}_t; \sqrt{\alpha_t}\mathbf{x}_0, (1 - \alpha_t)\mathbf{I}). \quad (2)$$

In this formulation, the sequence σ_t satisfies $0 < \sigma_1 < \dots < \sigma_{T-1} < \sigma_T < 1$.

The generation process in diffusion models is the reverse process. This process starts with pure Gaussian noise $\mathbf{x}_T \sim \mathcal{N}(\mathbf{x}_T; \mathbf{0}, \mathbf{I})$ and gradually reconstructing the data towards the original \mathbf{x}_0 . During the reverse process, each step $p_\theta(\mathbf{x}_{t-1}|\mathbf{x}_t)$ is modeled using a neural network.

$$p_\theta(\mathbf{x}_{1:T}) = p(\mathbf{x}_T) \prod_{t=1}^T p_\theta(\mathbf{x}_{t-1}|\mathbf{x}_t), \quad (3)$$

$$p_\theta(\mathbf{x}_{t-1}|\mathbf{x}_t) = \mathcal{N}(\mathbf{x}_{t-1}; \boldsymbol{\mu}_\theta(\mathbf{x}_t, t), \boldsymbol{\Sigma}_\theta(\mathbf{x}_t, t)), \quad (4)$$

$$p(\mathbf{x}_T) = \mathcal{N}(\mathbf{x}_T; \mathbf{0}, \mathbf{I}). \quad (5)$$

Typically, $\boldsymbol{\Sigma}_\theta$ is set as an untrainable, time-dependent constant, $\boldsymbol{\Sigma}_\theta(\mathbf{x}_t, t) = \sigma_t \mathbf{I}$. Additionally, with a change in the parameterization of $\boldsymbol{\mu}_\theta$, the reverse process $p_\theta(\mathbf{x}_{t-1}|\mathbf{x}_t)$ can be expressed as:

$$\begin{aligned} & p_\theta(\mathbf{x}_{t-1}|\mathbf{x}_t) \\ &= \mathcal{N}\left(\mathbf{x}_{t-1}; \frac{1}{\sqrt{\alpha_t}} \left(\mathbf{x}_t + \frac{\sigma_t^2}{\sqrt{\alpha_t} - 1} \boldsymbol{\epsilon}_\theta(\mathbf{x}_t, t)\right), \sigma_t \mathbf{I}\right), \end{aligned} \quad (6)$$

where $\bar{\alpha}_t = \prod_{i=1}^t (1 - \sigma_i^2)$. The term $\boldsymbol{\epsilon}_\theta(\mathbf{x}_t, t)$ represents a function that predicts the noise from noisy data \mathbf{x}_t . This parameterization results in an objective function for the DDPM structured as follows:

$$\mathbb{E}_{\mathbf{x}_0, \boldsymbol{\epsilon}, t} \left[\|\boldsymbol{\epsilon} - \boldsymbol{\epsilon}_\theta(\mathbf{x}_t, t)\|_2^2 \right], \quad (7)$$

where $\mathbf{x}_t = \sqrt{\bar{\alpha}_t}\mathbf{x}_0 + \sqrt{1 - \bar{\alpha}_t}\boldsymbol{\epsilon}$.

While numerous parameterizations are recognized, such as predicting the observed data \mathbf{x}_0 from its noisy counterpart \mathbf{x}_t or v-prediction ([Ho et al., 2022b](#); [Salimans & Ho, 2022](#); [Kingma et al., 2021](#)), we chose to utilize the $\boldsymbol{\epsilon}$ -prediction.

In terms of the architecture of diffusion models, 2D U-Net ([Ronneberger et al., 2015](#)) architectures are commonly used for image data. In 2D U-Net-based models, spatial attention layers are incorporated between the convolutional layers. These spatial attention layers enhance the ability to focus on relevant spatial features and improve the quality of the generated images. Although we adopted a U-Net-based architecture for the diffusion model, [Peebles & Xie \(2022\)](#) explored architectures based on Vision Transformers (ViT) ([Dosovitskiy et al., 2020](#)).

2.2. Architectures for Video Diffusion Models

To generate videos, diffusion models need to encapsulate both spatial and temporal features across frames. While DDPMs typically comprise a combination of U-Net and spatial attention layer, their capability is predominantly confined to spatial feature capture.

To address this limitation, Video Diffusion Models (VDMs) ([Ho et al., 2022b](#)) were introduced as an initial attempt into video generation using diffusion models. By incorporating mechanisms to capture temporal dynamics within DDPMs, VDMs enhance their capability to capture temporal features (Figure 1(a)). Temporal attention layer is commonly used in video generation diffusion models, such as VDMs, to leverage time-series dependencies. However, temporal attention requires memory proportional to the square of the sequence length, which imposes limitations on the maximum length of video sequences that can be generated at once.

In our study, we adopt VDMs as a baseline to explore the existing challenges and potential improvements in video generation using diffusion models.

3. Method

In this section, we propose the architecture of a temporal SSM (state-space model) layer for use in diffusion models for videos. Recent diffusion model-based video generation techniques capture temporal features through temporal attention layers, incurring memory costs proportional to

Module Type	Parallelizability	Memory Usage
RNN	×	BLD
Attention	✓	$B(L^2 + DL)$
Linear Attention	✓	$B(D^2 + DL)$
SSM	✓	BLD

Table 1. Comparison of time-series handling modules in terms of parallelization capability and memory usage related to batch size (B), sequence length (L) and hidden dimension (D).

the square of the sequence length. Recently, SSMs have emerged as a promising alternative to attention, offering linear memory costs with respect to the sequence length (Gu et al., 2020; 2021; 2022; Smith et al., 2023; Gu & Dao, 2023). We first review the recent advancements in SSMs in prior works, followed by a detailed description of our proposed temporal SSM layer architecture for video generation diffusion models.

3.1. State Space Models

Unlike the temporal attention commonly used in video diffusion models, state-space models (SSMs) enable the processing of time series with spatial complexities proportional to the sequence length. Recent studies proposed SSMs that could process inputs in parallel unlike recurrent models such as recurrent neural networks (RNNs) (Chung et al., 2014).

SSMs are widely used as sequence models that define a mapping from one-dimensional input signals $u_k \in \mathbb{R}$ to one-dimensional output signals $y_k \in \mathbb{R}$, with $s_k \in \mathbb{R}^D$ representing the hidden state. Discrete time sequences are processed as follows:

$$\mathbf{s}_k = \bar{\mathbf{A}}\mathbf{s}_{k-1} + \bar{\mathbf{B}}u_k, y_k = \bar{\mathbf{C}}\mathbf{s}_k, \quad (8)$$

where $\bar{\mathbf{A}} \in \mathbb{R}^{D \times D}$, $\bar{\mathbf{B}} \in \mathbb{R}^{D \times 1}$, $\bar{\mathbf{C}} \in \mathbb{R}^{1 \times D}$. Unlike RNNs but akin to attention mechanisms, linear SSMs are capable of parallel computations through discrete convolutions, facilitated by the Fast Fourier Transform. The memory requirements and parallelizability of the modules managing the time series data are concisely summarized in Table 1.

SSMs on their own are not a complete solution for sequence modeling. They become effective when the discrete-time matrices $\bar{\mathbf{A}}, \bar{\mathbf{B}}, \bar{\mathbf{C}}$ are derived from a suitable continuous-time state-space model, which enables them to efficiently manage long-range dependencies (Gu et al., 2020). In response, S4 (Gu et al., 2021) aims to learn the continuous-time SSM parameterization of $\mathbf{A}, \mathbf{B}, \mathbf{C}$ and the discretization rate Δ , utilizing these to derive the requisite discrete-time parameters. Due to the complexity of the original transformation process, Gu et al. (2022) introduced S4D as a simplified diagonalized version of S4 that maintains similar performance in handling long sequences. We chose

S4D as a backbone model for our temporal SSM layer.

As delineated in Equations 8, SSMs are inherently designed to independently handle single-input, single-output (SISO) systems. Therefore, when employing SSMs to manage multidimensional inputs, it is common practice to append a structure to capture dependencies (such as GLU (Dauphin et al., 2017)) between different dimensions of the output after the SSM (Gu et al., 2021; 2022) (see Figure 1 (c)).

3.2. Temporal SSM Layer for Diffusion Model-based Video Generation

We incorporate state-space models (SSMs) within the temporal layers for the video generation diffusion model. The structure of our proposed temporal SSM layer (Figure 1 (b)), is a key element of our study and warrants detailed discussion. This design takes cues from the structure of the temporal attention layer in VDMs, which consists of Layer Normalization (Ba et al., 2016) followed by an attention mechanism and a skip connection (He et al., 2016).

In our model, we replace the self-attention component with an SSM. We adopt a bidirectional structure, drawing from practices in Graves & Schmidhuber (2005); Wang et al. (2022); Yan et al. (2023). This choice is motivated by the inherent limitation of a single SSM, which is typically restricted to capturing unidirectional temporal transitions. By adopting a bidirectional approach, SSMs can more comprehensively understand the temporal dynamics in video data, addressing the constraints of traditional unidirectional SSMs.

Additionally, we recognize that SSM, while effective, has limitations in integrating information across different dimensions, demonstrated in Equation 8. To overcome this, we supplement the SSM with a multi-layer perceptron (MLP) after the bidirectional SSM module (Figure 1(b)). Our experiments demonstrate that this addition significantly enhances the model’s performance, proving its importance in the overall architecture.

Given an input $\mathbf{X} \in \mathbb{R}^{(B \times H \times W) \times L \times C}$, where L is sequence length, C is channel size, H is height, W is width of the input image, our proposed temporal SSM layer operates as follows:

$$\begin{aligned} \mathbf{H} &= \text{LayerNorm}(\mathbf{X}), \\ \mathbf{F} &= \text{GLU}(\text{SSM}_{\text{forward}}(\mathbf{H})), \\ \mathbf{B} &= \text{GLU}(\text{SSM}_{\text{backward}}(\text{Flip}(\mathbf{H}))), \\ \mathbf{U} &= \mathbf{F} + \text{Flip}(\mathbf{B}), \\ \mathbf{O} &= \text{MLP}(\mathbf{U}) + \mathbf{H}. \end{aligned}$$

The ‘Flip’ function is used to reverse the temporal order of the sequence for the backward SSM and then restore the original order after processing. Element-wise summation

is used to merge the forward and backward information flows, and the MLP serves to integrate across the channel dimension, which is empirically critical for performance.

4. Related Works

4.1. Deep Generative Models for Video Generation

The field of video synthesis has seen significant advancements through various studies. Prior to the emergence of diffusion models, the use of generative adversarial networks (GANs) (Goodfellow et al., 2014) dominated the scene. These methods extended traditional image-GAN frameworks to video generation, focusing on enhancing their generative capabilities (Vondrick et al., 2016; Saito et al., 2017; Tulyakov et al., 2018; Ge et al., 2022). These approaches primarily aimed to achieve their objectives by extending common architectures of GANs for image generation. Additionally, the development of long-term video generation techniques, particularly those leveraging the transitions of latent variables in variational autoencoders (VAEs) (Kingma & Welling, 2013) are also well-known. (Kim et al., 2019; Gregor & Besse, 2018; Saxena et al., 2021; Yan et al., 2021).

The advent of diffusion models in image generation (Sohl-Dickstein et al., 2015; Nichol & Dhariwal, 2021; Ho et al., 2020) marked a turning point, with their subsequent application to video distributions demonstrating promising outcomes (Ho et al., 2022b; Singer et al., 2022; Ho et al., 2022a; Harvey et al., 2022; Blattmann et al., 2023). These approaches have shown promising results. Nevertheless, the recent approaches adopt attention mechanisms to temporal layers, which requires memory proportional to the square of the sequence length, the computational and memory demands of video-diffusion models pose a substantial challenge. To mitigate this:

Spatiotemporal Downsampling Techniques like Singer et al. (2022) and Ho et al. (2022a) have been developed to reduce computational costs by lowering spatial resolution and temporal frequency while employing temporal attention layers for capturing temporal features. These methods complement our research, which concentrates on lightening the module that captures temporal dynamics.

Latent Diffusion Models Exploring latent diffusion models presents an alternative approach (Rombach et al., 2022), focusing on simpler latent variables rather than directly processing complex data (He et al., 2022). Some strategies involve using pre-trained image diffusion models with additional trainable layers for handling temporal features to lessen the overall computational load (Zhou et al., 2022; Blattmann et al., 2023).

Multistep Generation Schemes In the realm of long-term video prediction using video diffusion models, multistep

generation techniques are stand out (Voleti et al., 2022; Höpfe et al., 2022; Harvey et al., 2022; Yin et al., 2023). These schemes generates videos through successive sampling with flexible frame conditioning, allowing for efficient long-term dependency modeling with minimal memory usage. Our research diverges from them by focusing on architectural improvements rather than sampling schemes.

4.2. Structured State Space Sequence (S4) Models

Originally introduced in Gu et al. (2021), S4 represents a sequence modeling framework that first solved all tasks in the Long-Range Arena (Tay et al., 2021). At its core lies the structured parameterization of state-space models (SSMs), offering efficient computation and demonstrating outstanding performance, in capturing long-range dependencies (Gu et al., 2020; 2021). The mathematical foundation of S4 is complex, prompting recent efforts to demystify, simplify, and improve S4 (Gu et al., 2022; Smith et al., 2023; Gu & Dao, 2023). The S4D (Gu et al., 2022) used in our study is one of such developments.

S4 and its variants have been applied across various domains, including image and video classification (Nguyen et al., 2022; Knigge et al., 2023; Islam & Bertasius, 2022; Wang et al., 2023), segmentation (Ma et al., 2024), image representation learning (Liu et al., 2024), speech generation (Goel et al., 2022), time-series generation (Zhou et al., 2023), language modeling (Mehta et al., 2023; Wang et al., 2022; Dao et al., 2023), reinforcement learning (Bar David et al., 2023; Lu et al., 2023; Deng et al., 2023). In the field of diffusion models using SSMs, DiffuSSM (Yan et al., 2023) have explored the integration of SSMs with diffusion models, replacing the computationally intensive spatial attention mechanisms in image generation with SSMs. However, the application of SSMs in video generation diffusion models remains underexplored, an area our research aims to delve into and expand upon.

5. Experiments

In this section, we introduce the incorporation of temporal SSM layers as temporal layers in diffusion models for video generation. This method facilitates the generation of longer video sequences while maintaining generative performance, overcoming the limitations imposed by memory constraints in attention-based temporal layers of video diffusion models. To empirically validate our hypothesis, we conducted a series of experiments comparing our temporal SSM layer with the temporal attention layer in video diffusion models. We also compared temporal linear attention, which has a linear spatial complexity similar to our temporal SSM layer. Additionally, we conducted an ablation study to investigate the effectiveness of each component within our temporal SSM layer. Through this analysis, we aim to identify the

Dataset	UCF101		MineRL		
	16	16	64	200	400
# of Frames	16	16	64	200	400
Resolution	32×32	64×64	32×32	32×32	32×32
Attention	272.152	618.005	1073.339	1032.514	–
Linear Attention	285.995	670.776	1175.453	1170.834	1072.001
Our SSM	226.447	634.546	1132.982	1116.339	972.306

Table 2. Comparison of FVD in UCF101 and MineRL Navigate. The absence of values for generating 400 frames using the attention mechanism is attributed to the training on NVIDIA A100 exceeding the maximum memory capacity, rendering the experiment infeasible.

critical elements when integrating an SSM into the temporal layer of video diffusion models.

5.1. Experimental Setup

Datasets We used two datasets to compare the performance of the temporal layers under varying conditions. Training details for each dataset and each frame length are shown in Appendix A. UCF101 (Soomro et al., 2012) was selected as the standard video dataset. Following Ho et al. (2022b), 13,320 videos from the training and test sets were used. We sampled clips with frame lengths of 16 and downsampled their spatial resolution to 32×32 pixels or 64×64 pixels for manageability. Additionally, we incorporated MineRL Navigate dataset (Guss et al., 2019; Saxena et al., 2021), which includes 961 videos for training purposes. Each video has 500 frames. This choice was motivated by our aim to validate the model’s performance with longer video sequences. We explored 64, 200, and 400 frames length, and downsampled the spatial resolution to 32×32 pixels.

Baseline We established our experimental baseline using VDMs (Ho et al., 2022b). Our analysis was meticulously designed to alter only the temporal attention layers in VDMs with our temporal SSM layers. This strategy enabled a focused examination of the impact and efficacy of the temporal SSM layers in the context of video generation, facilitating a direct comparison with the existing temporal layers.

Evaluation Metrics In our validation process, we evaluated the sample quality of the videos generated by the trained models. To evaluate the quality of the generated videos, we employ the Fréchet Video Distance (FVD) metric (Unterthiner et al., 2018), using an I3D network pre-trained on the Kinetics-400 dataset (Carreira & Zisserman, 2017). FVD is a recognized standard for assessing the quality of generated videos (Ho et al., 2022b; Ge et al., 2022; Singer et al., 2022; Ho et al., 2022a; Harvey et al., 2022), where lower scores denote superior quality. For the UCF101 dataset, we evaluated FVD using all 13,320 videos and 10,000 generated samples. For the MineRL Navigate dataset, the calculation involves all 961 videos and 1,000 generated samples.

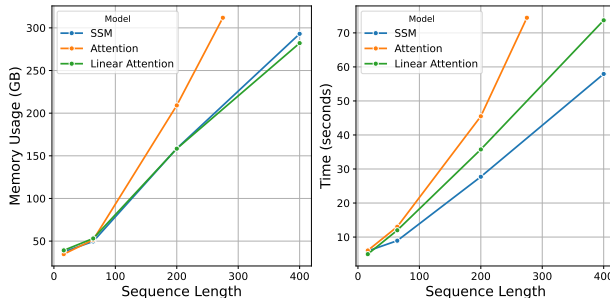


Figure 2. Left: Memory consumption during training with 8 NVIDIA A100 GPUs (40 GB) at a batch size of 8 and resolution of 32×32 . Right: Inference time for generating a sample with a single NVIDIA A100 GPU at a resolution of 32×32 and $T = 256$.

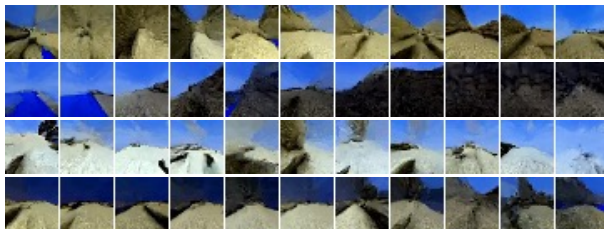


Figure 3. Qualitative results in MineRL Navigate (number of frames are 400). Each row represents a different sample, while each column corresponds to a sampling taken every 40 frames out of 400 frames.

5.2. Benchmark Results

We initially focus on a standard video benchmark of UCF101 to compare generative performance (measured using FVD) across different temporal layers. The quantitative results are in Table 2. The qualitative results of this generation are presented in Figure 4 (Appendix B). It is observed that the temporal SSM layer outperforms both temporal attention and temporal linear attention in generative performance in the 32×32 setting and performs competitively in the 64×64 setting.

We then utilize MineRL Navigate, a dataset with longer-term sequences, to observe the ability of temporal SSM

SSM	MLP		FVD	
	Bidirectional	# of Layers	Position	UCF101
✓	2	post	226.447	<u>1132.982</u>
✓	2	pre	<u>253.688</u>	1129.245
	2	post	669.582	1371.131
✓	1	post	267.935	1189.216
✓	0	–	269.811	1193.491

Table 3. Quantitative results of ablation studies in our temporal SSM layers with UCF101 16 frames and MineRL Navigate 64 frames.

layers to generate video sequences of lengths unattainable by temporal attention layers, while competitively maintaining generative performance. The transitions in these metrics as the video length increases are illustrated in Table 2. Additionally, qualitative results of the generated videos are shown in Figure 3.

In Figure 2, we present how training memory consumption and inference time vary with video sequence length for each temporal layer, using 32×32 resolution images. Training memory consumption data is based on a batch size of 8, while inference times reflect sample generation on a single NVIDIA A100 GPU with the number of diffusion time steps T fixed at 256. Notably, for the attention layer, experiments were capped at 275 frames instead of 400 due to memory limitations of the devices, which restrict training of attention-based video diffusion models to a maximum of approximately 275 frames.

While SSM exhibits competitive generative performance compared to temporal attention, it’s noteworthy that temporal attention encounters memory errors at sequence lengths 400, a limitation not faced by temporal SSM. This highlights SSM’s enhanced capability in handling longer sequences without compromising computational efficiency. Furthermore, SSM outperforms temporal linear attention in terms of generative performance. This finding underscores SSM’s superiority in its ability to generate high-quality videos in longer video generation.

5.3. Ablation Study of Temporal SSM Layers

In the pursuit of temporal SSM layer in video generation diffusion models, our empirical findings indicate a considerable influence of elements in the temporal layer’s architecture on model performance. We conduct an ablation study to investigate the effects of each component of temporal SSM layer (Figure 1 (b)).

Bidirectional SSM Switching from bidirectional SSM to unidirectional SSM leads to a significant reduction in generative performance (Table 3). This result show that the bidirectional usage of SSMs significantly improves the ability of temporal SSM layer to capture temporal relationships.

MLPs in Temporal SSM Layers In this section, we shall discuss the configuration of the MLP within our temporal SSM layer. The proposed temporal SSM layer is composed of a bidirectional SSM followed by a dual-layer MLP with GeLU activation (Hendrycks & Gimpel, 2016). The rationale behind placing the MLP after the bidirectional SSM was that the SSM part of bidirectional SSM is a single-input, single-output system that was incapable of extracting relationships with other dimensions of the input. Therefore, the MLP was used to enhance the extraction of relationships with other input dimensions.

Specifically, we compared the following configurations: placing the MLP before the bidirectional SSM rather than after, replacing the MLP with a single layer and removing the MLP altogether. The results are listed in Table 3. Transitioning from a dual-layer MLP to a single linear layer, and eventually eliminating all such components, consistently leads to a stepwise degradation in generative performance across two datasets. The results also reveal that the placement of a dual-layer MLP, whether before or after the SSM, does not significantly affect the generative capability. These findings imply that in video diffusion models employing a temporal SSM layer, the generative performance heavily relies on the expressive capacity of the temporal SSM layer, while the positioning of components relative to the SSM plays a less crucial role in determining performance.

5.4. Comparison with Prior SSM Architectures

Recent years have seen a surge in research efforts to apply SSMs across various domains, accompanied by the proposal of numerous SSM architectures. Within this burgeoning field of study, gated state-space (GSS) architectures have emerged as one of the effective structures (Mehta et al., 2023). For instance, in Wang et al. (2022), bidirectional gated SSM (BiGS) architectures are employed for language modeling and image generation (Wang et al., 2022; Yan et al., 2023). GSS and BiGS architectures are composed of single linear layers for linear transformation, SSMs, skip connections implemented through multiplication (gating), and a two-layer MLP.

Among other effective SSM architectures, the Mamba archi-

Architecture Settings			FVD	
Architectures	Bidirectional	Dims of MLPs	UCF101	MineRL-64
GSS		$d_{input} \times 3$	699.383	1683.820
BiGS	✓	$d_{input} \times 3$	<u>233.277</u>	1157.793
BiGS	✓	512	237.244	<u>1153.669</u>
Mamba		-	669.572	1722.097
Bi-Mamba	✓	-	275.416	1156.891
Bi-Mamba + MLP	✓	512	<u>243.638</u>	<u>1138.779</u>
Ours	✓	512	226.447	1132.982

Table 4. FVD Comparison with SSM layers proposed in prior works across UCF101 16 frames and MineRL Navigate 64 frames. The resolution of both datasets is 32×32 pixels. The dimensionality of the input processed by the temporal layer, d_{input} , is equal to the channel size, C , as inferred from the dimensions of the input tensor $\mathbf{X} \in \mathbb{R}^{(B \times H \times W) \times L \times C}$. In the experimental settings described in this table, the channel sizes in the upper layers of the UNet architecture follow a sequential order of 64, 128, 256, and 512, starting from the topmost layer and progressing downwards.

ecture has been proposed (Gu & Dao, 2023). The Mamba architecture is characterized by a structure that alternates between 1D Convolution and SSM, and when combined with an SSM known as S6 (Gu & Dao, 2023), it has been applied to language understanding and learning of visual representations (Wang et al., 2024; Liu et al., 2024). For the learning of visual representations, a bidirectional version of Mamba, referred to here as Bi-Mamba, has also been proposed (Zhu et al., 2024). The architectures of these bidirectional SSM layers, which are more complex compared to our proposed temporal SSM layer.

It is important to note that in this section, with the goal of ensuring a fair comparison of architectures, the experiments with GSS, BiGS, Mamba, and Bi-Mamba all utilize the S4D as the SSM, similar to our temporal S4D layer. Architecture details are shown in Appendix C.

The comparisons between GSS and BiGS, as well as between Mamba and Bi-Mamba, suggest that the incorporation of bidirectionality significantly contributes to the capability of generating videos, a phenomenon not limited to our temporal SSM layers. Furthermore, introducing a Multilayer Perceptron (MLP) with a number of hidden layer dimensions that do not depend on the input size, following the SSM layer as done in our temporal SSM layers, to both BiGS and Bi-Mamba architectures, has been observed to result in performance improvements in some cases.

Then, we compare the generative performance of these structures and our proposed temporal SSM layer when used as the temporal layer in VDMs. The results indicate that, even when bidirectionality is applied and the size of the MLP’s hidden layers is aligned with ours, these models exhibit inferior generative performance compared to our simple temporal SSM layer. A potential reason for this discrepancy is that while GSS, BiGS, Mamba and Bi-Mamba focus on

language and image modeling using solely the SSM layers, our study seeks a temporal SSM layer specifically tailored to capture the temporal features of video, making the former approaches excessively redundant for this purpose.

6. Discussion

Our experimental findings demonstrate that incorporating SSM into the temporal layers of diffusion models for video generation offers superior video modeling in terms of memory efficiency for handling increased sequence lengths compared to traditional models employing temporal attention, while maintaining competitive generative quality. It is empirically shown that, while attention-based video generation diffusion models struggle to generate longer videos due to memory constraints, SSM-based video diffusion models are capable of producing such videos. These outcomes underscore the adaptability of temporal SSM layers in enhancing video diffusion models and indicate their extensive potential impact on the future advancements in this domain.

This study paves the way for numerous future investigations. While we have verified the advantages of employing our temporal SSM layers within the architecture of VDMs, the application of our temporal SSM layers extends beyond this, to any model that employs temporal attention for temporal dimension. For example, adopting temporal SSM layers into the temporal components of architectures such as Make-A-Video (Singer et al., 2022) or Imagen Video (Ho et al., 2022a) could further enhance their computational efficiency by leveraging their existing spatiotemporal downsampling mechanism. Additionally, the combination of the temporal SSM layers with Latent Diffusion Models (Rombach et al., 2022) could lead to significant reductions in computational costs. Our findings also offer insights for methods that involve freezing pretrained image-generation diffusion models

and training new temporal layers for video generation; simply substituting these newly inserted temporal layers with the SSM layers could be an effective strategy. Moreover, while our experiments concentrated on unconditional video generation, integrating our approach with conditional generation techniques such as classifier guidance (Dhariwal & Nichol, 2021) and classifier free guidance (Ho & Salimans, 2022) could pave the way for more efficient text-to-video (T2V) models.

The results of this study indicate that the incorporation of SSMs can lead to the development of long-term video generation models that demand fewer memory resources. This has noteworthy implications for broadening the accessibility of cutting-edge research in video generation diffusion models. Even institutions with limited computational resources can engage in this advanced field, potentially expediting the pace of research and innovation in video generation.

Impact Statement

This paper presents work whose goal is to advance the field of Machine Learning. There are many potential societal consequences of our work, none which we feel must be specifically highlighted here.

References

- Ba, J. L., Kiros, J. R., and Hinton, G. E. Layer normalization. *arXiv preprint arXiv:1607.06450*, 2016.
- Bar David, S., Zimerman, I., Nachmani, E., and Wolf, L. Decision s4: Efficient sequence-based rl via state spaces layers. In *International Conference on Learning Representations*, 2023.
- Blattmann, A., Rombach, R., Ling, H., Dockhorn, T., Kim, S. W., Fidler, S., and Kreis, K. Align your latents: High-resolution video synthesis with latent diffusion models. In *CVPR*, 2023.
- Carreira, J. and Zisserman, A. Quo vadis, action recognition? a new model and the kinetics dataset. In *CVPR*, 2017.
- Chung, J., Gulcehre, C., Cho, K., and Bengio, Y. Empirical evaluation of gated recurrent neural networks on sequence modeling. *arXiv preprint arXiv:1412.3555*, 2014.
- Dao, T., Fu, D. Y., Saab, K. K., Thomas, A. W., Rudra, A., and Ré, C. “hungry hungry hippos: Towards language modeling with state space models”. In *The International Conference on Learning Representations (ICLR)*, 2023.
- Dauphin, Y. N., Fan, A., Auli, M., and Grangier, D. Language modeling with gated convolutional networks. In *International conference on machine learning*, pp. 933–941. PMLR, 2017.
- Deng, F., Park, J., and Ahn, S. Facing off world model backbones: Rnns, transformers, and s4. *arXiv:2307.02064*, 2023.
- Dhariwal, P. and Nichol, A. Diffusion models beat gans on image synthesis. *arXiv preprint arXiv:2105.05233*, 2021.
- Dosovitskiy, A., Beyer, L., Kolesnikov, A., Weissenborn, D., Zhai, X., Unterthiner, T., Dehghani, M., Minderer, M., Heigold, G., Gelly, S., et al. An image is worth 16x16 words: Transformers for image recognition at scale. *arXiv preprint arXiv:2010.11929*, 2020.
- Elfwing, S., Uchibe, E., and Doya, K. Sigmoid-weighted linear units for neural network function approximation in reinforcement learning. *Neural Networks*, 107:3–11, 2018.
- Ge, S., Hayes, T., Yang, H., Yin, X., Pang, G., Jacobs, D., Huang, J.-B., and Parikh, D. Long video generation with time-agnostic vqgan and time-sensitive transformer. *arXiv preprint arXiv:2204.03638*, 2022.
- Goel, K., Gu, A., Donahue, C., and Ré, C. It’s raw! audio generation with state-space models. In *International Conference on Machine Learning*, 2022.
- Goodfellow, I., Pouget-Abadie, J., Mirza, M., Xu, B., Warde-Farley, D., Ozair, S., Courville, A., and Bengio, Y. Generative adversarial nets. In *Advances in Neural Information Processing Systems*, pp. 2672–2680, 2014.
- Graves, A. and Schmidhuber, J. Framewise phoneme classification with bidirectional lstm and other neural network architectures. *Neural Networks*, 18(5-6):602–610, 2005.
- Gregor, K. and Besse, F. Temporal difference variational auto-encoder. *arXiv preprint arXiv:1806.03107*, 2018.
- Gu, A. and Dao, T. Mamba: Linear-time sequence modeling with selective state spaces. *arXiv preprint arXiv:2312.00752*, 2023.
- Gu, A., Dao, T., Ermon, S., Rudra, A., and Ré, C. Hippo: Recurrent memory with optimal polynomial projections. *Advances in Neural Information Processing Systems*, 33: 1474–1487, 2020.
- Gu, A., Goel, K., and Ré, C. Efficiently modeling long sequences with structured state spaces. *arXiv preprint arXiv:2111.00396*, 2021.
- Gu, A., Goel, K., Gupta, A., and Ré, C. On the parameterization and initialization of diagonal state space models. In *Advances in Neural Information Processing Systems*, volume 35, pp. 35971–35983, 2022.

- Guss, W. H., Houghton, B., Topin, N., Wang, P., Codel, C., Veloso, M., and Salakhutdinov, R. Miner1: A large-scale dataset of minecraft demonstrations. *arXiv preprint arXiv:1907.13440*, 2019.
- Harvey, W., Naderiparizi, S., Masrani, V., Weilbach, C., and Wood, F. Flexible diffusion modeling of long videos. *arXiv preprint arXiv:2205.11495*, 2022.
- He, K. et al. Deep residual learning for image recognition. In *Proceedings of the IEEE conference on computer vision and pattern recognition*, 2016.
- He, Y. et al. Latent video diffusion models for high-fidelity long video generation. *arXiv preprint arXiv:2211.13221*, 2022.
- Hendrycks, D. and Gimpel, K. Gaussian error linear units (gelus). *arXiv preprint arXiv:1606.08415*, 2016.
- Ho, J. and Salimans, T. Classifier-free diffusion guidance. *arXiv preprint arXiv:2207.12598*, 2022.
- Ho, J., Jain, A., and Abbeel, P. Denoising diffusion probabilistic models. In *Advances in Neural Information Processing Systems*, pp. 6840–6851, 2020.
- Ho, J., Chan, W., Saharia, C., Whang, J., Gao, R., Gritsenko, A., Kingma, D. P., Poole, B., Norouzi, M., Fleet, D. J., et al. Imagen video: High definition video generation with diffusion models. *arXiv:2210.02303*, 2022a.
- Ho, J., Salimans, T., Gritsenko, A., Chan, W., Norouzi, M., and Fleet, D. J. Video diffusion models, 2022b.
- Hochreiter, S. and Schmidhuber, J. Long short-term memory. *Neural computation*, 9(8):1735–1780, 1997.
- Höppe, T. et al. Diffusion models for video prediction and infilling. *arXiv preprint arXiv:2206.07696*, 2022.
- Islam, M. M. and Bertasius, G. Long movie clip classification with state-space video models. In *ECCV*, 2022.
- Kim, T., Ahn, S., and Bengio, Y. Variational temporal abstraction. In *Advances in Neural Information Processing Systems*, pp. 11566–11575, 2019.
- Kingma, D. P. and Welling, M. Auto-encoding variational bayes. *International Conference on Learning Representations*, 2013.
- Kingma, D. P., Salimans, T., Poole, B., and Ho, J. Variational diffusion models. *arXiv preprint arXiv:2107.00630*, 2021.
- Kitaev, N., Kaiser, L., and Levskaya, A. Reformer: The efficient transformer. In *International Conference on Learning Representations*, 2020. URL <https://openreview.net/forum?id=rkgNKkHtvB>.
- Knigge, D. M., Romero, D. W., Gu, A., Gavves, E., Bekkers, E. J., Tomczak, J. M., Hoogendoorn, M., and Sonke, J.-j. Modelling long range dependencies in nd: From task-specific to a general purpose cnn. In *International Conference on Learning Representations*, 2023.
- Liu, Y., Tian, Y., Zhao, Y., Yu, H., Xie, L., Wang, Y., Ye, Q., and Liu, Y. Vmamba: Visual state space model. *arXiv preprint arXiv:2401.10166*, 2024.
- Lu, C., Schroecker, Y., Gu, A., Parisotto, E., Foerster, J., Singh, S., and Behbahani, F. Structured state space models for in-context reinforcement learning. *arXiv preprint arXiv:2303.03982*, 2023.
- Ma, J., Li, F., and Wang, B. U-mamba: Enhancing long-range dependency for biomedical image segmentation. *arXiv preprint arXiv:2401.04722*, 2024.
- Mehta, H., Gupta, A., Cutkosky, A., and Neyshabur, B. Long range language modeling via gated state spaces. In *The Eleventh International Conference on Learning Representations*, 2023.
- Nguyen, E., Goel, K., Gu, A., Downs, G., Shah, P., Dao, T., Baccus, S., and Ré, C. S4nd: Modeling images and videos as multidimensional signals with state spaces. In *Advances in Neural Information Processing Systems*, 2022.
- Nichol, A. Q. and Dhariwal, P. Improved denoising diffusion probabilistic models. In *International Conference on Machine Learning*, pp. 8162–8171. PMLR, 2021.
- Peebles, W. and Xie, S. Scalable diffusion models with transformers. *arXiv preprint arXiv:2212.09748*, 2022. doi: 10.48550/arXiv.2212.09748.
- Rombach, R., Blattmann, A., Lorenz, D., Esser, P., and Ommer, B. High-resolution image synthesis with latent diffusion models. In *Proceedings of the IEEE/CVF conference on computer vision and pattern recognition*, pp. 10684–10695, 2022.
- Ronneberger, O., Fischer, P., and Brox, T. U-net: Convolutional networks for biomedical image segmentation. In *International Conference on Medical Image Computing and Computer-Assisted Intervention*, pp. 234–241. Springer, 2015.
- Saito, M., Matsumoto, E., and Saito, S. Temporal generative adversarial nets with singular value clipping. In *IEEE International Conference on Computer Vision (ICCV)*, 2017.
- Salimans, T. and Ho, J. Progressive distillation for fast sampling of diffusion models. In *International Conference on Learning Representations (ICLR)*, 2022.

- Saxena, V., Ba, J., and Hafner, D. Clockwork variational autoencoders. *Advances in Neural Information Processing Systems*, 34, 2021.
- Shen, Z., Zhang, M., Zhao, H., Yi, S., and Li, H. Efficient attention: Attention with linear complexities. *CoRR*, abs/1812.01243, 2018. URL <http://arxiv.org/abs/1812.01243>.
- Singer, U., Polyak, A., Hayes, T., Yin, X., An, J., Zhang, S., Hu, Q., Yang, H., Ashual, O., Gafni, O., et al. Make-a-video: Text-to-video generation without text-video data. *arXiv:2209.14792*, 2022.
- Smith, J. T., Warrington, A., and Linderman, S. Simplified state space layers for sequence modeling. In *International Conference on Learning Representations*, 2023.
- Sohl-Dickstein, J., Weiss, E., Maheswaranathan, N., and Ganguli, S. Deep unsupervised learning using nonequilibrium thermodynamics. In *International Conference on Machine Learning*, pp. 2256–2265, 2015.
- Song, Y., Sohl-Dickstein, J., Kingma, D. P., Kumar, A., Ermon, S., and Poole, B. Score-based generative modeling through stochastic differential equations. *arXiv preprint arXiv:2011.13456*, 2021. doi: 10.48550/arXiv.2011.13456.
- Soomro, K., Zamir, A. R., and Shah, M. Ucf101: A dataset of 101 human actions classes from videos in the wild. *arXiv preprint arXiv:1212.0402*, 2012. doi: 10.48550/arXiv.1212.0402.
- Tay, Y., Dehghani, M., Abnar, S., Shen, Y., Bahri, D., Pham, P., Rao, J., Yang, L., Ruder, S., and Metzler, D. Long range arena: A benchmark for efficient transformers. In *International Conference on Learning Representations*, 2021.
- Tulyakov, S., Liu, M.-Y., Yang, X., and Kautz, J. Mocogan: Decomposing motion and content for video generation. In *Proceedings of the IEEE conference on computer vision and pattern recognition*, pp. 1526–1535, 2018.
- Unterthiner, T., van Steenkiste, S., Kurach, K., Marinier, R., Michalski, M., and Gelly, S. Towards accurate generative models of video: A new metric challenges. *arXiv preprint arXiv:1812.01717*, 2018.
- Vaswani, A., Shazeer, N., Parmar, N., Uszkoreit, J., Jones, L., Gomez, A. N., Kaiser, Ł., and Polosukhin, I. Attention is all you need. In *Advances in Neural Information Processing Systems*, pp. 5998–6008, 2017.
- Voleti, V., Jolicoeur-Martineau, A., and Pal, C. Mcvd-masked conditional video diffusion for prediction, generation, and interpolation. In *Advances in neural information processing systems*, volume 35, pp. 23371–23385, 2022.
- Vondrick, C., Pirsivash, H., and Torralba, A. Generating videos with scene dynamics. In *Advances in Neural Information Processing Systems (NeurIPS)*, 2016.
- Wang, J., Yan, J. N., Gu, A., and Rush, A. M. Pretraining without attention. *arXiv preprint arXiv:2212.10544*, 2022.
- Wang, J., Zhu, W., Wang, P., Yu, X., Liu, L., Omar, M., and Hamid, R. Selective structured state-spaces for long-form video understanding. In *CVPR*, 2023.
- Wang, J. et al. Mambabyte: Token-free selective state space model. *arXiv preprint arXiv:2401.13660*, 2024.
- Wang, S., Li, B. Z., Khabsa, M., Fang, H., and Ma, H. Linformer: Self-attention with linear complexity, 2020.
- Yan, J. N., Gu, J., and Rush, A. M. Diffusion models without attention. *arXiv preprint arXiv:2311.18257*, 2023.
- Yan, W. et al. Videogpt: Video generation using vq-vae and transformers. *arXiv preprint arXiv:2104.10157*, 2021.
- Yin, S. et al. Nuwa-xl: Diffusion over diffusion for extremely long video generation. *arXiv preprint arXiv:2303.12346*, 2023.
- Zhou, D. et al. Magicvideo: Efficient video generation with latent diffusion models. *arXiv preprint arXiv:2211.11018*, 2022.
- Zhou, L., Poli, M., Xu, W., Massaroli, S., and Ermon, S. Deep latent state space models for time-series generation. In *International Conference on Machine Learning*, 2023.
- Zhu, L. et al. Vision mamba: Efficient visual representation learning with bidirectional state space model. *arXiv preprint arXiv:2401.09417*, 2024.

A. Details in Benchmark Experiments

To ensure a fair comparison of the modules extracting the temporal relationships under the same resolution settings, all configurations except for the temporal layers, were the same in our experiments. We used NVIDIA V100 $\times 4$ or NVIDIA A100 $\times 8$ (from a cloud provider). Detailed configuration is shown in Table 5.

Dataset	UCF101		MineRL		
	16	16	64	200	400
# of Frames	16	16	64	200	400
Resolution	32×32	64×64	32×32	32×32	32×32
Base channel size	64	64	64	64	64
Channel multipliers	1, 2, 4, 8	1, 2, 4, 8	1, 2, 4, 8	1, 2, 4, 8	1, 2, 4, 8
Time embedding dimension	1024	1024	1024	1024	1024
Time embedding linears	2	2	2	2	2
# of attention heads (for attentions)	8	8	8	8	8
Dims of attention (for attentions)	64	64	64	64	64
SSM hidden dims (for SSMs)	512	512	512	512	512
MLP hidden dims (for SSMs)	512	512	512	512	512
Denoising timesteps (T)	256	1000	256	256	256
Loss type	L2 loss of ϵ	L2 loss of ϵ	L2 loss of ϵ	L2 loss of ϵ	L2 loss of ϵ
Training steps	92k	106k	174k	255k	246k
Optimizer	Adam	Adam	Adam	Adam	Adam
Training learning rate	0.0003	0.0001	0.0003	0.0003	0.00005
Train batch size	64	64	8	8	8
EMA decay	0.995	0.995	0.995	0.995	0.995
GPUs	V100 $\times 4$	A100 $\times 8$	V100 $\times 4$	A100 $\times 8$	A100 $\times 8$
Training Time	72 hours	120 hours	72 hours	100 hours	120 hours

Table 5. Experimental Setup for UCF101, MineRL Navigate datasets.

B. Additional Qualitative Results



Figure 4. Qualitative generation results in UCF101 (# of frames are 16, 64×64 resolution).

C. Details of Architectures in Prior Works

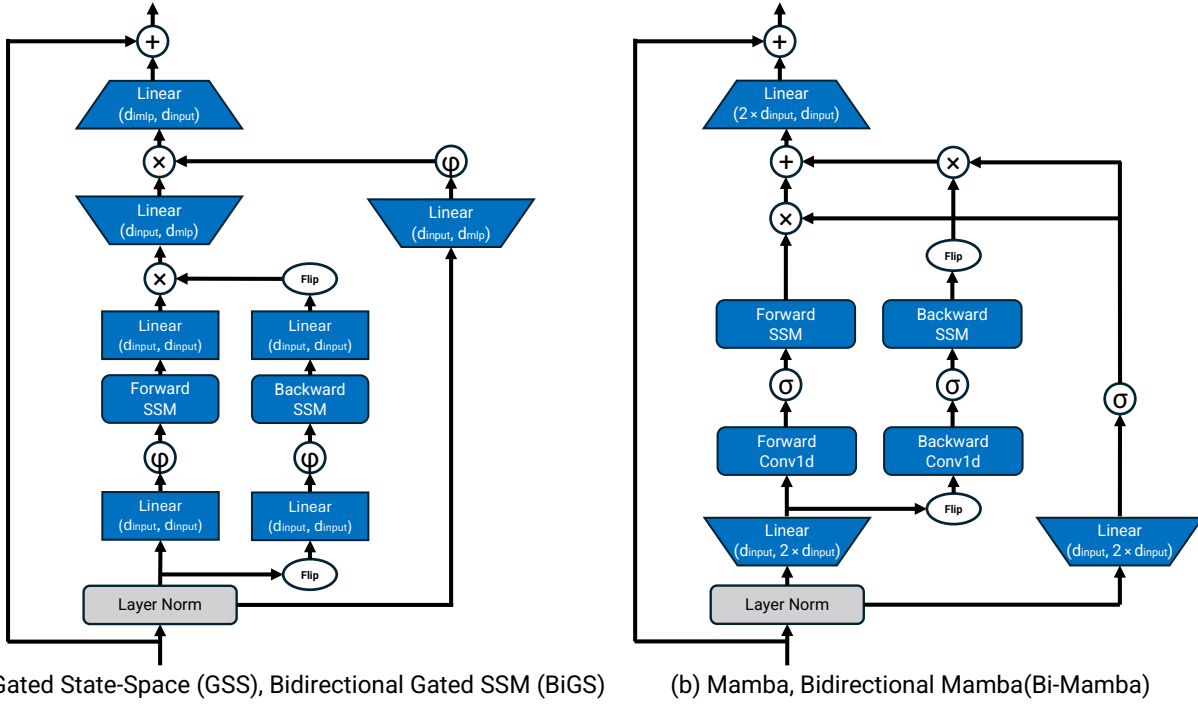


Figure 5. Details of architectures in prior works (Mehta et al., 2023; Wang et al., 2022; Gu & Dao, 2023; Zhu et al., 2024). ⊕ means element-wise summation and ⊗ means element-wise product. Ⓢ means GeLU activation (Hendrycks & Gimpel, 2016) and Ⓢ means SiLU activation (Elfving et al., 2018). In “Bi-Mamba + MLP” experiments in Section 5.3, we replaced the last linear layer in Bi-Mamba with a two-layer MLP.